doi:10.1016/j.jmb.2004.03.028 J. Mol. Biol. (2004) 339, 145–159

JMB

Available online at www.sciencedirect.com

SCIENCE DIRECT®

ELSEVIER

Unique Physicochemical Profile of β-Amyloid Peptide Variant Aβ1–40E22G Protofibrils: Conceivable Neuropathogen in Arctic Mutant Carriers

A. Päiviö[1,2], J. Jarvet[3], A. Gräslund[3], L. Lannfelt[4] and A. Westlind-Danielsson[1,5]*

[1]*Department of NEUROTEC Karolinska Institutet, Geriatric Medicine, Novum KFC, SE-141 86 Huddinge, Sweden*

[2]*Department of Molecular Biosciences, Swedish University of Agricultural Sciences, The Biomedical Centre, P.O. Box 575, SE-751 23 Uppsala, Sweden*

[3]*Department of Biochemistry and Biophysics, The Arrhenius Laboratories, University of Stockholm, SE-106 91 Stockholm, Sweden*

[4]*Department of Public Health and Caring Sciences/Geriatrics Rudbeck Laboratory, Uppsala University, SE-751 85 Uppsala Sweden*

[5]*Disease Biology, Drug Discovery Unit, H. Lundbeck A/S, 9 Ottiliavej, DK-2500 Valby, Denmark*

**Corresponding author*

A new early-onset form of Alzheimer's disease (AD) was described recently where a point mutation was discovered in codon 693 of the β-amyloid (Aβ) precursor protein gene, the Arctic mutation. The mutation translates into a single amino acid substitution, glutamic acid → glycine, in position 22 of the Aβ peptide. The mutation carriers have lower plasma levels of Aβ than normal, while *in vitro* studies show that Aβ1–40E22G protofibril formation is significantly enhanced. We have explored the nature of the Aβ1–40E22G peptide in more detail, in particular the protofibrils. Using size-exclusion chromatography (SEC) and circular dichroism spectroscopy (CD) kinetic and secondary structural characteristics were compared with other Aβ1–40 peptides and the Aβ12–28 fragment, all having single amino acid substitutions in position 22. We have found that Aβ1–40E22G protofibrils are a group of comparatively stabile β-sheet-containing oligomers with a heterogeneous size distribution, ranging from >100 kDa to >3000 kDa. Small Aβ1–40E22G protofibrils are generated about 400 times faster than large ones. Salt promotes their formation, which significantly exceeds all the other peptides studied here, including the Dutch mutation Aβ1–40E22Q. Position 22 substitutions had significant effects on aggregation kinetics of Aβ1–40 and in Aβ12–28, although the qualitative aspects of the effects differed between the native peptide and the fragment, as no protofibrils were formed by the fragments. The rank order of protofibril formation of Aβ1–40 and its variants was the same as the rank order of the length of the nucleation/lag phase of the Aβ12–28 fragments, E22V > E22A ≫ E22G > E22Q ≫ E22, and correlated with the degree of hydrophobicity of the position 22 substituent. The molecular mass of peptide monomers and protofibrils were estimated better in SEC studies using linear rather than globular calibration standards. The characteristics of the Aβ1–40E22G suggest an important role for the peptide in the neuropathogenesis in the Arctic form of AD.

Keywords: amyloid; protofibrils; Arctic mutation; kinetics; Alzheimer's disease

Present address: Anita Westlind-Danielsson, Disease Biology, H. Lundbeck A/S, 9 Ottiliavej, DK-2500 Valby, Copenhagen, Denmark.

Abbreviations used: AD, Alzheimer's disease; ADDL, amyloid-derived diffusible ligands; βAPP, β-amyloid precursor protein; PS, presenilin; Aβ, β-amyloid; EM, electron microscopy; AFM, atomic-force microscopy; DAD, diode array detector; PB, phosphate buffer; PBS, phosphate-buffered saline; SEC, size-exclusion chromatography; V_0, void volume; V_e, elution volume; M_{Glob}, molecular mass calculated using global protein standards; M_{Dex}, molecular mass calculated using dextran standards; P, protofibrils.

E-mail address of the corresponding author: awd@lundbeck.com

Introduction

A number of single-nucleotide mutations in the β-amyloid peptide (Aβ) coding region of the β-amyloid precursor protein (βAPP) have been reported that cause single amino acid substitutions clustering around codon 693 (positions 692–694) of βAPP that can cause early-onset familial forms of Alzheimer's disease (AD). The resultant Aβ peptides are: A21G (the Flemish variant);[1] E22Q (Dutch);[2,3] E22K (Italian);[4] E22G (Arctic);[5] and D23N (Iowa).[6] Codon 693 of βAPP encodes the glutamic acid residue through the GAG nucleotide triplet. Single-nucleotide mutations in this codon encode the Dutch (CAG), Italian (AAG) and Arctic (GGG) mutations. There are three other possible position 22 single-nucleotide mutations that could lead to early-onset AD: valine E22V (GTG); alanine E22A (GCG); and aspartic acid (GAT and GAC).

The pathological expression of the clinically relevant Aβ variants share common features and show distinct clinical as well as neuropathological characteristics. Cerebral amyloid angiopathy is a common clinical denominator and dementia another, with one exception. The Dutch mutation carriers suffer from hereditary cerebral haemorrhage with amyloidosis Dutch-type (HCHWA-D) where dementia is not so common but, if present, does not seem to be of the AD type but conforms better to vascular dementia.[7] Vascular Aβ deposition contains mainly Aβ1–40 and brain Aβ1–40 levels by far exceed those of Aβ1–42 in these mutation carriers where this has been examined.[8–11] Interestingly Aβ1–40 levels dominate senile plaques from Flemish mutation carriers, whereas the Dutch mutation carriers have no detectable plaque-bound Aβ1–40.[8] Neurofibrillary tangles are present to various extents in these Aβ diseases;[6,8] they are scarce or completely lacking.[12,13] The fibrillogenic properties of these Aβ peptides have, in all five cases, been found to be changed.[5,14–19] This change may affect the production,[20,21] deposition, proteolytic susceptibility,[22] clearance rates[23] and cellular toxicity[17,24–27] of Aβ *in vivo*. In-depth examination of these steps may result in a deeper insight as to how seemingly subtle changes in the primary sequence of Aβ translates into dramatic changes in Aβ metabolism and furthermore into distinct neuropathology and clinical expression of the disease.

The Aβ peptide is produced by the sequential proteolysis of βAPP by β and γ-secretase.[28] Provided concentrations become high enough,[29] monomeric random coil Aβ polymerizes into β-sheet-containing fibrils that, in turn, deposit as senile plaques. In the process, small oligomeric intermediates are formed, followed by larger so-called protofibrils,[30,31] protofilaments and fibrils. Some oligomeric Aβ species, such as amyloid-derived diffusible ligands, ADDLs,[32] seem to be an end stage of a structurally distinct group of oligomeric Aβ1–42 species that do not readily go on to form fibrils.[33] Protofibrils, on the other hand, do form fibrils but in a manner that is still not well understood. The morphology of protofibrils is distinct from that of ADDLs[32] and Aβ fibrils.[30,31,34,35] Protofibrils have been reported to affect several electrical properties of neurons in culture,[36,37] effects that could well undermine normal impulse propagation in the brain. Protofibril-mediated toxicity to primary neuronal cultures[17,34] has been reported. Although the potential neuropathophysiological relevance of the oligomeric and protofibrillar Aβ species in Aβ diseases is largely unknown, there is growing concern that these, and not so much Aβ plaques, play a significant role in the pathogenesis of familial and sporadic AD.

In vitro fibrillization studies of the recently reported Arctic mutation established a significantly enhanced formation and build-up of protofibrillar species of Aβ1–40E22G.[5] Arctic mutant carriers show early-onset progressive AD with attenuated plasma levels of Aβ1–40 and Aβ1–42. We previously hypothesized that the high rate of protofibril formation and potential build-up in the brain may lead to a number of deleterious effects on neuronal function and survival, promoting the early Arctic AD phenotype.[5] In order to understand better how this could evolve, we set out to further explore the Arctic Aβ1–40 peptide variant in more detail using size-exclusion chromatography (SEC) and circular dichroism spectroscopy (CD). A number of kinetic, biophysical and chemical properties associated with the Arctic Aβ1–40E22G monomers and protofibrils were examined together with the native peptide, an extension of prior observations,[5] and comparisons were made with four other Aβ1–40 peptides containing position 22 substitutions, Q, K, A and V. Mutations producing AβE22A and E22V are not known to have clinical association. The position 22 substitutions were investigated in the Aβ12–28 fragment that, in some respects, provides an easier model peptide to work with. Some comparisons were also made with Aβ1–40A21G.

Results

General

The primary sequence of Aβ, from amino acid residues 12–28, is illustrated in Figure 1 together with all the amino acid substitutions studied in this work. The molecular mass of Aβ1–40E22G peptide is 72 Da less than the native peptide (4258 Da *versus* 4330 Da) and the calculated isoelectric point (pI) of the peptide is somewhat higher than that of the native peptide (5.7 *versus* 5.2). The Arctic peptide loses a negative charge at neutral pH. Glycine is considerably more hydrophobic than glutamic acid.

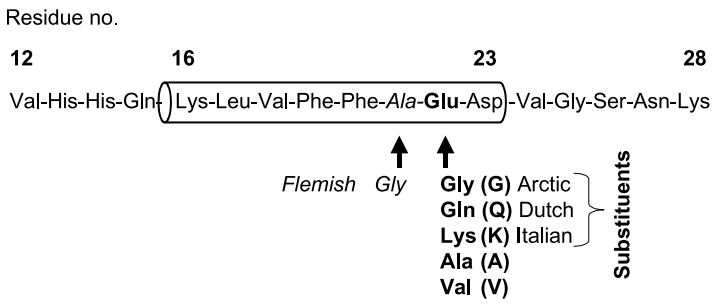

Figure 1. Amino acid sequence for Aβ12–28 with the position 21 and 22 substitutions. The Aβ peptide position 21 and 22 substitutions used in this study are illustrated in the primary sequence 12–28 fragment and, where appropriate, with their relevant clinical designations. The bold-face amino acid substituents have been examined in both Aβ1–40 and Aβ12–28, whereas the substituent in italics has been studied only in Aβ1–40 (Flemish). The predicted α-helix for the Aβ1–40 peptide is indicated with a schematic cylinder drawn between amino acid residues 16 and 23.

Chromatographic properties

Aβ1–40 and Aβ1–40E22G monomers and protofibrils

In Table 1, the elution volumes (V_e) of the peptides are given. They differ by 35 μl, where Aβ1–40E22G is the slightly delayed peptide. The V_e values of the protofibrillar peptide peaks differ by 24 μl (Table 1), Aβ1–40E22G having a V_e of 0.957 ml and Aβ1–40 of 0.981. Results from four separate kinetic experiments carried out for 47–70 hours showed a significant reduction in V_e for the Aβ1–40 and Aβ1–40E22G protofibrillar peaks with time of either peptide, suggesting that there is a time-dependent growth in protofibrillar size (not shown).

Aβ12–28 fragments

Distinct elution volumes, V_e, were observed for all of the Aβ12–28 fragments (Table 3). These were found to correlate ($R^2 = 0.94$) with the hydrophobicity of the free L-amino acid in position 22 (Figure 2) but not with the size of the peptide fragment. The more hydrophobic the substitution, the larger the V_e. The hydrophobicity values used here for the free amino acids are scaled values from computational log(P) determinations by the small fragment approach.[38]

Molecular mass determinations

Aβ1–40 and Aβ1–40E22G monomers and protofibrils

Table 2 gives the estimated molecular mass values for monomer and protofibrils along with the calculated number of molecules per estimate, determined using three chromatographic columns with different separation ranges. Calibration was carried out using either four globular proteins or seven dextran standards (see Materials and Methods). Molecular mass values determined using the former standards are given as M_{Glob} and those determined using the latter are given as M_{Dex}. Chromatograms from separations on each of the three columns showed a peak overlapping with the void volume (V_0) as well as a monomeric peak, which is more delayed the larger the separation range of the column. Also, the larger the fractionation range for the column, the higher and the longer was the plateau seen between the two peaks, which most likely represents a size continuum of smaller oligomeric species. From separations on three columns, M_{Glob} values for Aβ1–40E22G protofibrils were found to range from $>1.82 \times 10^5$ Da to $>29 \times 10^6$ Da and contain anywhere from >40 to >7000 peptide molecules. The M_{Glob} values of the monomeric peaks calculated in this manner are twice the values for the actual monomeric peptide species. In contrast, the M_{Dex} of the freshly dissolved peptides comes very close to their actual monomeric molecular mass (Table 2). Estimations of the M_{Dex} values for the three different size groups of protofibrils separated with the three different columns show an increased number of peptides: >24 (Superdex 75 column), >117 (Superdex 200) and >692 (Superose 6) molecules, respectively.

Aβ12–28 fragments

The molecular mass values for the Aβ12–28

Table 1. Elution volumes (V_e) for protofibril and monomeric SEC peaks for Aβ1–40 and Aβ1–40E22G using a Superdex 75 column

Chromatographic peak	Aβ1–40		Aβ1–40E22G		Difference in	
	V_e (ml)	n	V_e (ml)	n	V_e (ml)	P value
Protofibril	0.981 ± 0.003	56	0.957 ± 0.003	57	0.024	<0.001
Monomer	1.609 ± 0.003	55	1.644 ± 0.005	56	0.035	<0.001

The values, mean ± SEM, are calculated from 113 injections from four separate kinetic experiments each carried out over 48 hours. The P values were determined using an unpaired Student's t-test.

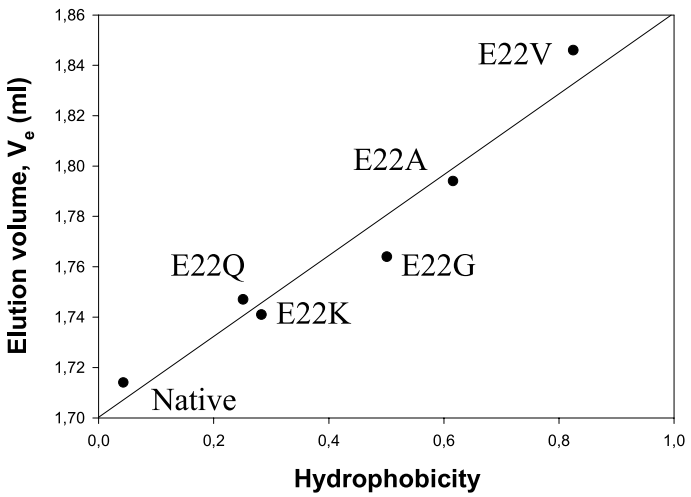

Figure 2. Correlation of Aβ12–28 peptide elution volume with position 22 amino acid substituent hydrophobicity. The calculated hydrophobicity values for the free L-amino acids were used.[37]

peptide fragments, based on the dextran calibration standards, approach the actual monomeric mass values, similar to what is found with the full-length peptides (Table 3). When they contain very hydrophobic position 22 amino acid residues, such as G, V and A, they tend to deviate more from their actual molecular mass. Calculations using the globular standards, however, overestimate the value three to five times. Mass spectrometry confirmed the monomeric form of the fragments upon dissolution (data not shown).

Rate constants of fibril formation

The formation of Aβ1–40E22G protofibrils was found to be concentration-dependent (not shown). The rate of formation of three separate groups of Aβ1–40E22G (100 μM) protofibrils with sizes of >103, >500 and >3000 kDa were estimated during 336 minutes using the three different columns described in Table 2. Linear regression analysis of the initial 125–250 minutes showed that the group with a larger fraction of small protofibrils (>100 kDa) are formed at a considerably higher rate than those where larger protofibrillar sizes dominate (>500 kDa and >3000 kDa) (Figure 3). This is not surprising, as the local concentrations of Aβ plummet when small Aβ forms are consumed in the protofibrillar growth process. The relative rates of protofibril formation compared to Superdex 75 (= 1.0) were 0.351 (Superdex 200) and 0.026 (Superose 6). Comparatively few protofibrils have been formed at 336 minutes with a mass of >3000 kDa (Figure 3, the two bottom curves). The formation of the small group was estimated to be approximately 400 times faster than that for the large size group.

Structural analysis

Aβ1–40E22G and Aβ1–40

The CD spectra for Aβ1–40E22G and Aβ1–40 were recorded using four different peptide concentrations, 21, 50, 77 and 130 μM, measured at various time intervals up to six hours for Aβ1–40E22G and 48 hours for Aβ1–40. Spectra for Aβ1–40E22G, at 50 and 130 μM, are shown in Figure 4A and B. For the 50 μM peptide at time zero, the CD spectrum shows a minimum at 195 nm, typical of random coil secondary structure. After 60 minutes, a β-sheet-like spectrum with a minimum at 217 nm dominates. For the 130 μM peptide, the structural transition is almost complete at time zero (within few minutes). At 60 minutes, the shape of the CD spectrum indicates almost complete β-sheet structure; however, with a gradual loss of signal intensity. The loss of CD signal after longer incubation times is most likely due to optical inhomogeneity of the sample caused by formation of large aggregate particles. At 21 μM, random coil dominates for at least six hours. At 77 μM, the conversion to β-sheet conformation was, similar to 130 μM, almost complete within ten minutes. Similar protofibril CD spectra indicating β-sheet have been reported by Walsh *et al*. for fractions of protofibrils in native Aβ1–40 isolated by high-pressure liquid chromatography (HPLC).[30,37]

CD spectra for the native peptide (50 μM and 130 μM) show typical random coil structure (Figure 4C and D). The spectra were stable for at least 48 hours. SEC analysis after four days revealed no change (not shown).

In Figure 5 the kinetic changes of the monomeric (top curve, filled boxes) and protofibrillar peaks for Aβ1–40E22G (77 μM) are plotted together with the time-dependent change in molar ellipticity at 195 nm and 217 nm. These data show that the growing β-sheet like structure is accompanied by growth in the population of peptide oligomers and protofibrils.

Aβ1–40E22K

Random coil structure is the dominating secondary structure of the Italian Aβ1–40E22K for

Table 2. Calculation of molecular mass of monomeric Aβ1−40E22G and Aβ1−40 and protofibrils using SEC

	Column											
	Superdex 75				Superdex 200				Superose 6			
	($r = 0.987$)		($r = 0.979$)		($r = 0.994$)		($r = 0.999$)		($r = 0.991$)			
	Globular protein stds	M_{Obs}/M_{Calc}	Dextran stds	M_{Obs}/M_{Calc}	Globular protein stds	M_{Obs}/M_{Calc}	Dextran stds	M_{Obs}/M_{Calc}	Globular protein stds	M_{Obs}/M_{Calc}	Dextran stds	M_{Obs}/M_{Calc}
Monomeric (M_r)												
Aβ1−40E22G	8966	2.1	4236	1.00	9152	2.1	(a)		8624	2.0	(a)	
Aβ1−40	10,207	2.4	4857	1.12	n.d.	n.d.	(a)		n.d.	n.d.	(a)	
Protofibrils (M_r)												
Aβ1−40E22G	>182,000	43	>103,000	24	$>3.7 \times 10^6$	869	>500,000	117	$>29 \times 10^6$	6890	$>3 \times 10^6$	692
Aβ1−40	>182,000	42	>103,000	24	n.d.	n.d.	n.d.	n.d.	n.d.	n.d.	n.d.	n.d.

Relative molecular mass (M_r) calculations for Aβ1−40E22G and Aβ1−40 monomer and protofibrils using three different gel-filtration columns having different fractionation ranges. These ranges were dependent on the nature of the standard set. Superdex 75 (globular standards, 3000−70,000 Da; dextran standards, 1000−70,000 Da); Superdex 200 (globular stds. 10,000−600,000 Da; dextran stds. 10,000−500,000 Da); Superose 6 (globular standards, $5000-5 \times 10^6$ Da; dextran standards, $5000-5 \times 10^6$ Da). Correlation coefficients are given in parentheses under the column type. The number of peptide molecules observed (Obs) from SEC analysis is calculated by dividing by calculated molecular mass (M_{Calc}) (a). Smaller than the fractionation range. n.d., not determined.

Table 3. Molecular mass determination for Aβ12–28 fragments using a Superdex 75 column with six different amino acid substitutions in position 22. Free L-amino acid substituent hydrophobicity value, retention volume, nucleation phase length, mean residual ellipticity at 195 nm and their observed secondary structures

Aβ12–28 fragment	M_r (Da)	M_{Dex} (Da)	M_{Dex}/M_r	M_{Glob} (Da)	M_{Glob}/M_r	Amino acid hydrophobicity[37]	Retention volume V_e (ml)	Nucleation phase length (200 μM)	Molar ellipticity $[\theta] \times 10^{-3}$ (deg cm^2 dmol^{-1})	Secondary structure
Aβ12–28E22	1955	2362	1.21	10,700	5.47	0.043	1.714	>10 days	−4.0	Random coil
Aβ12–28E22G	1883	1985	1.02	9500	4.86	0.501	1.764	3.7 ± 1.0 hours	−9.5	Random coil
Aβ12–28E22Q	1954	1816	0.96	8900	4.73	0.251	1.747	5 days	−2.5	Random coil
Aβ12–28E22K	1954	2048	1.05	9700	4.96	0.283	1.741	6.8 ± 1.8 days	−17.0	Random coil
Aβ12–28E22A	1897	1550	0.82	8000	4.72	0.616	1.794	<20 minutes	4.0	β-Sheet
Aβ12–28E22V	1925	1179	0.61	6600	3.43	0.825	1.846	<20 minutes	13.5	β-Sheet

M_{Dex}, molecular mass calculations based on the dextran standards. M_{Glob} molecular mass calculations based on the globular protein standards.

at least two days at 50 μM (Figure 6A). A time-dependent decline was recorded however. The SEC data show an initial rapid fall in monomer levels within the first 24 hours followed by a slower decline, with no detectable levels of protofibrils (Figure 6B).

Aβ1–40E22A

No random coil structure was discernible in the CD studies of the Aβ1–40E22A peptide, but a typical β-sheet structure is recorded from time zero which is stable for at least three days (Figure 6C). The SEC data show a rapid drop in monomer levels with a parallel formation of protofibrils (Figure 6D). The protofibrils are consumed within 24 hours.

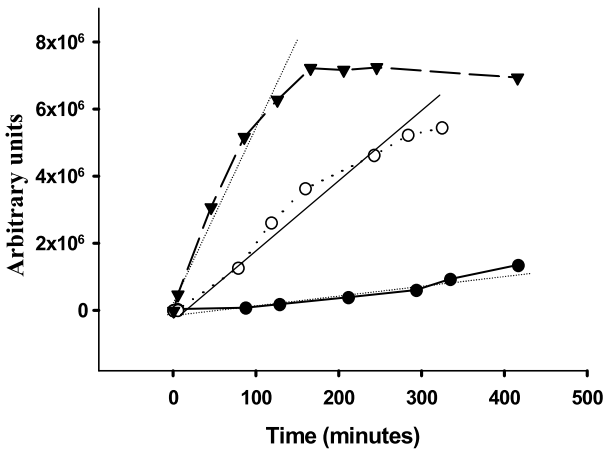

Figure 3. Kinetics of three Aβ1–40E22G protofibrillar size groups estimated using SEC and three different types of SEC columns. The protofibrillar peak measured as a function of time, integrated from SEC separations using Superdex 75, Superdex 200 and Superose 6 columns (see Table 2). Initial rate of formation (right). The top curve shows the rate of formation of Aβ species >100,000, >500,000 (middle) and 3.10^6 Da (bottom).

Aβ1–40E22V

The CD spectra of the valine-substituted peptide resembles Aβ1–40E22A and the spectra are almost superimposable (Figure 6C and E). The drop in monomeric levels is faster than for E22A (Figure 6D and F).

Aβ12–28

CD spectra for the Aβ12–28 fragments (200 μM) were measured up to 24 hours. Table 3 gives the mean residual ellipticity of the fragment at 195 nm, five minutes after dissolution, and the major secondary structure. Aβ12–28, Aβ12–28E22Q and Aβ12–28E22K exhibit mainly random coil structure up to 24 hours and Aβ12–28E22A and Aβ12–28E22V mainly β-sheet structure. The Aβ12–28E22G fragment showed a conformational change from random coil to β-sheet secondary structure within 24 hours.

To compare the kinetics of the Aβ12–28 fragments, the duration of the nucleation/lag phase was measured; i.e. the time passed prior to seeing a drop in the monomeric peak, the so-called aggregation/elongation phase.[29] The peptides displayed a wide range of lag phase lengths prior to aggregation. Under these conditions, the Aβ12–28E22V and Aβ12–28E22A were found to nucleate within 20 minutes. Estimations from CD studies showed the lag phase to be even shorter (less than five minutes) (Table 3). The rank order of nucleation was found to be Aβ12–28E22G > E22Q > E22K with lag phase times of 3.7 hours, 5.0 days and 6.75 days, respectively. The native fragment showed no tendency to aggregate up to almost four weeks. No protofibrils could be detected for any of the Aβ12–28 fragments, even at a concentration of 400 μM.

Kinetics of protofibril formation

Aβ1–40E22Q

The Dutch Aβ1–40E22Q peptide resembles

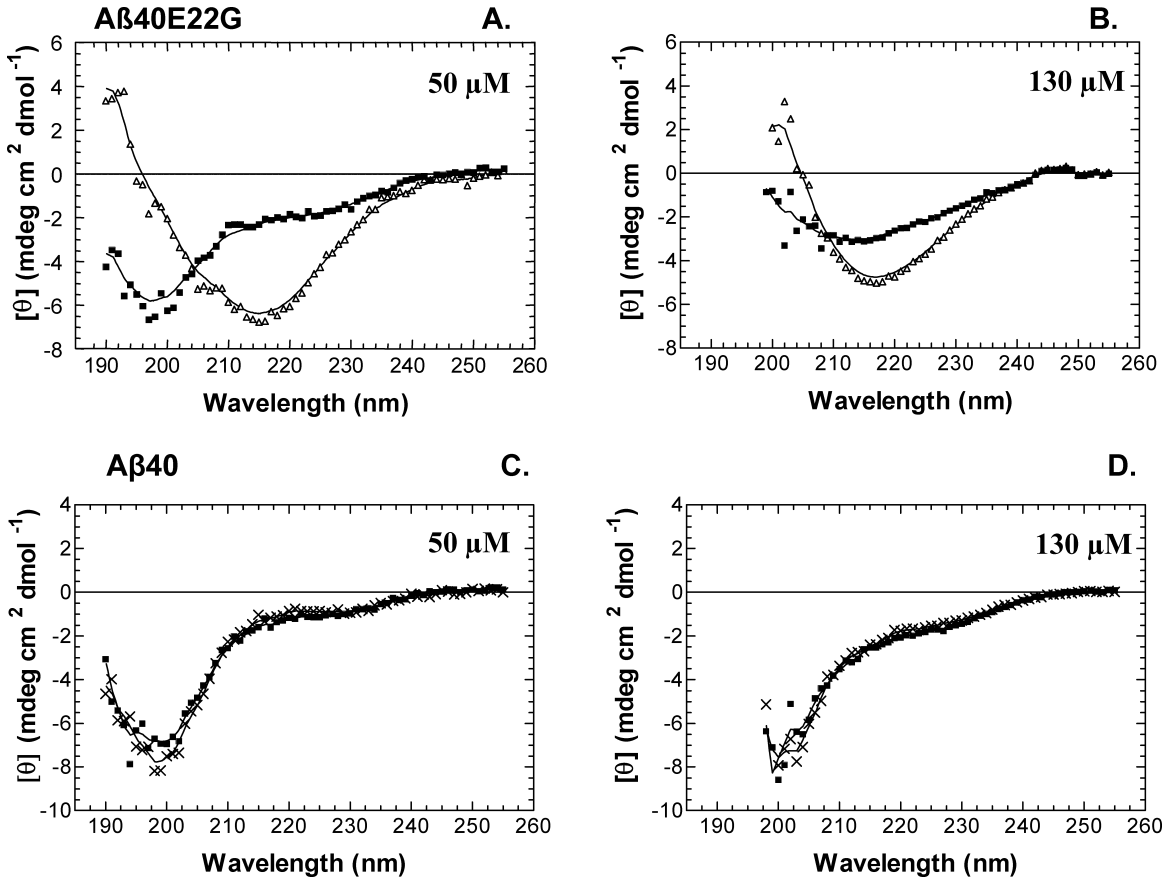

Figure 4. Time-dependent secondary structural changes for Aβ1–40E22G and Aβ1–40 analysed using circular dichroism. Circular dichroism spectra of (A) 50 μM and 130 μM (B) Aβ1–40E22G recorded in 50 mM phosphate buffer without NaCl (as chloride ions interfere with the CD analysis) at pH 7.4 at time zero (filled boxes) and at 60 minutes (open triangles). Circular dichroism spectra of C 50 μM and D 130 μM Aβ1–40 both at time zero (filled boxes) and at 60 hours (X).

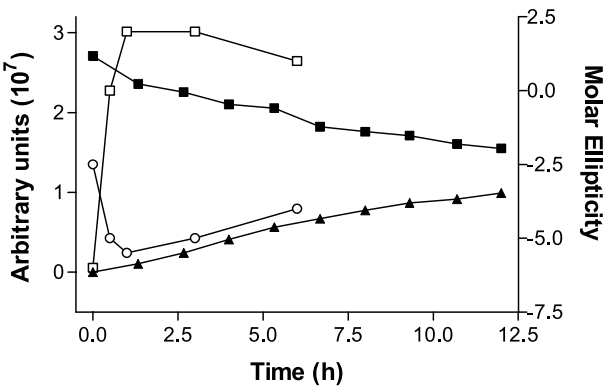

Figure 5. Circular dichroism and SEC for Aβ1–40E22G, run in parallel. The Figure illustrates the time-dependence of mean residual ellipticity at 195 nm (open boxes) and 217 nm (open circles), and time-dependent monomeric decline (filled boxes) and concomitant increase in protofibrillar levels (filled triangles). CD and SEC were measured at a peptide concentration of 77 μM and recordings were made from 0–6.5 hours (CD) and 0–12.5 hours (SEC).

Aβ1–40E22G in the kinetic studies (Figure 7A and B). With the addition of 0.1 M NaCl, Aβ1–40E22Q monomer levels drop to about half their initial concentration within a half-a-day, and protofibrils are formed in parallel. Without salt supplementation the process is restrained, resembling the effect of NaCl withdrawal on the Arctic variant, although NaCl seems to have a somewhat more pronounced effect on Aβ1–40E22G aggregation.

Aβ1–40E22G versus Aβ1–40E22Q, Aβ1–40A21G and Aβ1–40E22G : Aβ1–40 (1 : 1)

Protofibril formation of Aβ1–40E22G was compared directly to that of Aβ1–40E22Q in three separate experiments (Figure 8(A)). Although the initial rate of formation did not differ significantly between the two peptides at a concentration of 50 μM, the Aβ1–40E22G produced twice as high protofibril levels as the Aβ1–40E22Q.

The rate of protofibril formation of 50 μM Aβ1–40, Aβ1–40E22G, Aβ1–40A21G and a 1 : 1 mixture of Aβ1–40 and Aβ1–40E22G was compared in three separate experiments. One representative experiment is shown in Figure 8B. Very little or no Aβ1–40 or Aβ1–40A21G protofibrils were

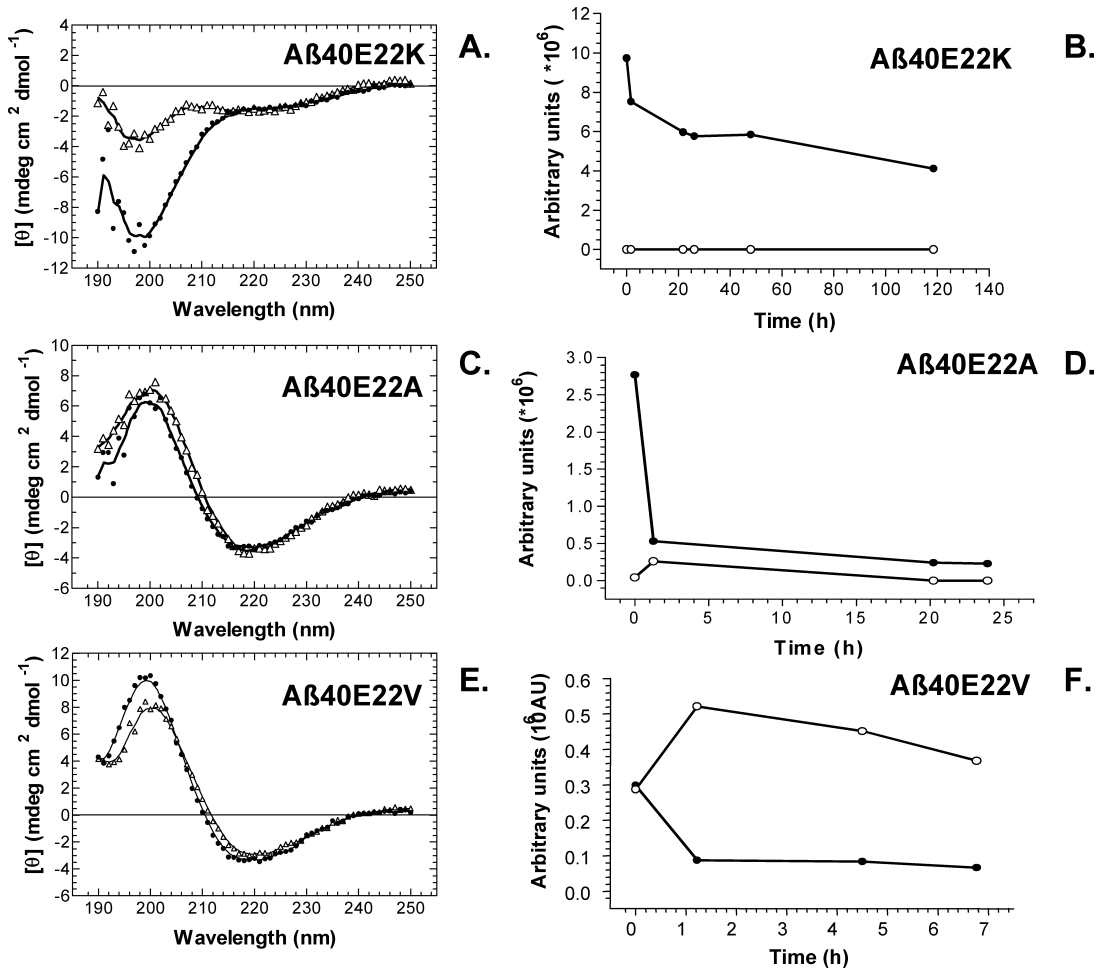

Figure 6. Circular dichroism and SEC analysis of Aβ1–40E22K, E22A and E22V. CD spectral measurements (A, C and E) at time zero (filled circles) to 60 minutes (open triangles) and SEC analyses (B, D and F) of monomer (filled circles) and protofibrillar peaks (open circles) of (A and B) Aβ1–40E22K, (C and D) Aβ1–40E22A, and (E and F) Aβ1–40E22V.

detected for at least 12.5 hours. The 1 : 1 Aβ1–40 : Aβ1–40E22G mixture showed a formation rate intermediate to Aβ1–40 and Aβ1–40E22G peptides as reported earlier.[5]

Protofibril stability

Aβ1–40 and Aβ1–40E22G

The stability of Aβ1–40E22G protofibrils was measured by collecting the SEC peak fraction of protofibrils that had reached maximal protofibril concentrations after 24 hours incubation (see the first two bars in Figure 9). The ratio of protofibrils (*P*)/monomer (3.05) in the initial sample is indicated to the right of the two bars. Immediately after collection, the samples were diluted 1 : 10 (v/v) with buffer (30 °C). After dilution, the aliquots were loaded onto the column and analysed at five different timepoints. Within 4.5 hours there is a decline of the *P*/monomer ratio to half the initial value. A stable equilibrium is then established for up to 22 hours. Similar findings were observed with a 1 : 5 dilution, although protofibrillar precipitation became significant at ten hours. With a 1 : 100 dilution, no protofibrils could be detected, only monomers were seen, even at the earliest time-point of 0.6 hour. Diluting Aβ1–40 peptide 1 : 10 dissociated protofibrils so that only the monomer could be detected at all time-points studied.

Discussion

On the basis of earlier observations, it has been suggested that synthetic Aβ1–40 (≤100 μM) dissolved in water at pH 7.4, exists predominantly as a dimer. These findings are based mainly on observations where SEC and globular protein calibration standards have been used.[39–42] We have extended these observations using three different gel-filtration columns, with distinct separation ranges, and globular calibration standards. We find that linear dextran polymers (95% unbranched) have much better molecular

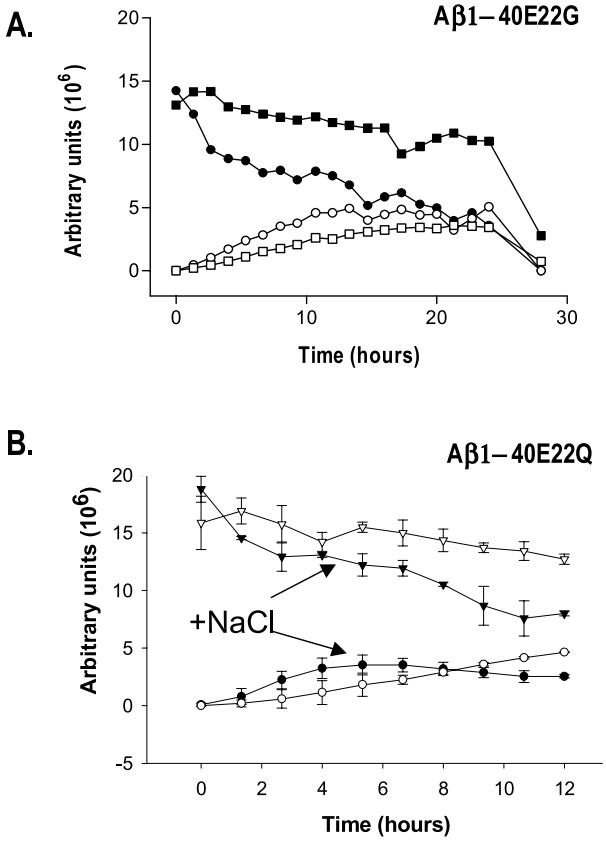

Figure 7. Kinetics of Aβ1–40E22G and Aβ1–40E22Q monomeric decline and protofibril formation in the absence or in the presence of 0.1 M NaCl supplementation. The initial peptide concentration was 40–50 μM. Monomeric (filled symbols) and protofibrillar (open symbols) formation was measured without (boxes) or with (circles) NaCl supplementation for Aβ1–40E22G ($n = 1$, representative of three) (A) and Aβ1–40E22Q (SEM ± SD; $n = 2$) (B). Note that the *X*-axis is not the same for A and B.

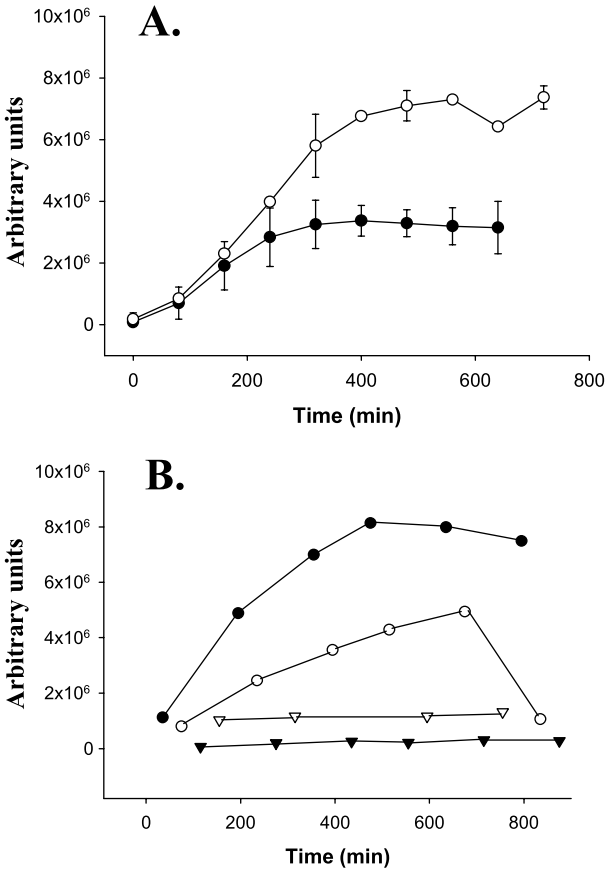

Figure 8. Protofibril formation of Aβ1–40E22Q and Aβ1–40A21G. A, The formation of Aβ1–40E22Q (filled circles; $n = 3$) protofibrils compared to that of Aβ1–40E22G (open circles; $n = 1$ or 3), both at a concentration of 77 μM in 50 mM PBS. Each point is the mean ± SD, except where no standard deviations are shown for Aβ1–40E22G (where there is only one value). B, Protofibril formation of Aβ1–40A21G (open triangles), Aβ1–40E22G (filled circles), Aβ1–40E22G : Aβ1–40 (1 : 1) (open circles), Aβ1–40 (filled triangles) were compared in parallel in three separate experiments. The curves are the result of one experiment representative of three.

mass prediction values as calibration standards for freshly dissolved Aβ1–40, Aβ1–40E22G as well as for fragments of Aβ1–40, such as Aβ12–28 and even Aβ15–25. The Aβ1–40 monomeric protein behaves more as a linear than a globular protein. Our studies show that the use of globular standards significantly overestimates the molecular mass, best exemplified by the results from experiments with the Aβ12–28 fragments (three- to fivefold overestimation). Based on the dextran standard calibration, our results suggest that the Aβ1–40, Aβ1–40E22G and Aβ12–28 peptides are mainly monomeric immediately after dissolution. Electrospray ionization Fourier transform ion cyclotron resonance mass spectrometry, a technique by which early Aβ oligomerization steps can be followed,[43] has shown that monomer levels were at least fourfold higher than dimer levels were in freshly dissolved Aβ1–40 solutions (100 μM) (M. Palmblad & J. Bergquist, personal communication). Previous findings using other techniques, including analytical ultracentrifugation,[44] nuclear magnetic resonance[45–47] or sedimentation analysis,[48] have concluded monomeric Aβ to be the major peptide form in freshly dissolved solutions.

Molecular mass estimates (>100 kDa) of protofibrils, based on SEC and the use of globular protein calibration standards, have been reported. Problems with non-ideal chromatographic behaviour of the Aβ were reported in these studies[30] and when reproduced by others.[49] Our estimated mass values for Aβ1–40E22G protofibrils, using dextran standards, are >103– > 3000 kDa, harbouring some >24– > 700 peptide molecules, respectively. The upper size limit of protofibrils is a function of the gravitational force in the centrifugation step used

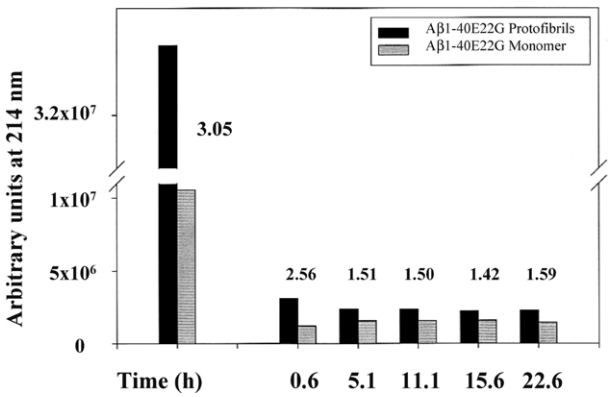

Figure 9. Stability measure of Aβ1–40E22G protofibrils collected from SEC compared to Aβ1–40 protofibrils. The protofibrillar (*P*) fraction from SEC was collected from Aβ1–40 and Aβ1–40E22G after 24 hours incubation. Collected samples were analysed immediately using SEC (time zero). These samples were then diluted 1 : 10 (v/v) and analysed at various time-points. The fraction *P*/monomer is given above the bars. No Aβ1–40 protofibril could be detected after the 1 : 10 dilution.

to separate these from large aggregates and fibrils prior to SEC analysis.

While the Aβ1–40E22G monomeric peak appeared at a later time-point than the Aβ1–40 peak on the chromatograms, as expected (Aβ1–40E22G $M_r = 4258$ *versus* 4330 for Aβ1–40), the opposite was true for the protofibrils. The shift in elution order of the native and Aβ1–40E22G protofibrils is probably due to the larger size of the Aβ1–40E22G protofibrils (see below), or alternatively, is due to non-ideal chromatographic behavior. However, in the case of the two monomers, although they elute in the right order, the difference in elution volume suggests that their M_r values differ by 723 and not by 72. This discrepancy could be explained by the possibility that the Aβ1–40E22G peptide interacts with the column gel matrix where the peptide is being retained either by charge attraction or, more likely, by hydrophobic interactions. The high salt concentration of the elution buffer (0.15 M) should normally prohibit peptide–gel matrix interactions, but this does not seem to be the case. When examining the chromatographic properties of the Aβ12–28 fragments, we found a clear correlation between the hydrophobicity of the amino acid substituent and the V_e, where the most hydrophobic fragments, and not the largest ones, were retained longer in the column.

The kinetic studies of protofibril formation allowed us to follow both the increment in protofibrillar levels as well as the growth in size with time. Numerous HPLC runs using the Superdex 75 column confirmed size growth as a shift of the protofibrillar peak to the left with time. This shift was larger for the Aβ1–40E22G than the native peak, and may be a function of the considerably higher stability and quicker formation these protofibrils show compared to the native protofibrils (Figure 9). These observations agree with the morphological size estimates from our past electron microscope (EM) studies of negative stain protofibrils, Aβ1–40E22G being longer than Aβ1–40.[5] When comparing kinetic studies on Superdex 75 with Superdex 200 and Superose 6, we could confirm the observations of a time-dependent size increment and, in addition, calculate how rapidly small, medium and large protofibrils form (Figure 3). A time-dependent increase in protofibrillar size is corroborated by earlier findings on the native peptide showing: (i) a size increment in Aβ1–40 protofibrils by way of linear extension, using atomic-force microscopy (AFM);[35] (ii) and an increase in the mean hydrodynamic radius of Aβ1–40 protofibrils with incubation time.[34]

The parallel CD and SEC observations of time-dependent structural and kinetic measurements of Aβ1–40E22G (Figure 5) were designed to allow direct time comparisons using the two different techniques. Prior to CD measurement, samples were diluted in ice-cold, double-distilled water. This has proven an effective means of dissolving Aβ peptides, removing possible aggregates that may have effects on kinetic experiments. Experiments show that low temperatures promote 3_1 helix formation in β peptides, a structure that inhibits further aggregation.[50] Thus samples were not centrifuged prior to CD measurements. Removal of NaCl from the incubation buffer was a prerequisite for the measurements, since CD is incompatible with the presence of Cl^-. As we observed in the SEC experiments, addition of NaCl (0.1 M) promotes the consumption of Aβ monomers to the advantage of increased rates and levels of protofibril formation (Figure 7A and B). The CD findings translate into a rapid concentration-dependent aggregation and high β-sheet content for Aβ1–40E22G protofibrils (Figures 4A and B and 5), where β-sheet structure clearly evolves in Aβ species smaller than protofibrils. Such aggregation was even more pronounced for the Aβ1–40E22A and Aβ1–40E22V variants (Figure 6D–F). For the latter peptide, the drop in monomer levels, seen on the SEC chromatograms, significantly exceeds that of the Aβ1–40E22A variant. A comparison of the SEC data for Aβ1–40E22G and Aβ1–40E22Q show large similarities and both display a more moderate drop in monomeric levels and concomitant increase in protofibril levels than the Aβ1–40E22A and Aβ1–40E22V. Aβ1–40E22G protofibril levels were found to exceed those of the Dutch variant peptide in this study, although their initial rates of formation were similar. Previous CD studies on the Dutch Aβ1–40E22Q have reported β-sheet structure,[17,19] and the results strongly resemble the data we have recorded for Aβ1–40E22G.[50] In contrast, Aβ1–40E22K does not produce any detectable level of protofibrils during the time-frames

examined, while the CD measurements show that the initial 195 nm spectral minimum disappears within five to six days and remains that way for at least another five days. These findings support previous reports of slow formation of Aβ1–40E22K fibrils.[17,19]

The Aβ12–28 fragment is known to form fibril aggregates and exert cellular toxicity *in vitro*.[51,52] Such fibrils have been shown in the past to closely resemble fibrils isolated from senile plaques of AD brains.[53,54] Depending on concentration, this fragment is mainly random coil or β-sheet structure in aqueous solution at higher temperatures,[55] and may exist in an ordered left-handed 3_1 helix conformation at low temperatures.[50] For the aggregation studies of the fragments, we registered the length of the time that elapsed prior to seeing a drop in the monomeric peak on the chromatogram, called the lag or nucleation phase. Examination of SEC and CD data from Aβ1–40 and its variants reveal that the rank order of β-sheet/protofibril formation is the same as the rank order of the lag phase for the Aβ12–28 fragments: E22V ≥ E22A ≫ E22G > E22Q ≫ E22, and correlated with the position 22 substituent free amino acid hydrophobicity (Figure 2). Furthermore, experiments with Aβ12–28 fragments reveal that the Aβ1–40E22G mutant has important N and/or C-terminal interactions that are necessary for protofibril generation/build-up, as Aβ12–28E22G protofibrils were not detected. In fact, none of the position 22 substituted Aβ12–28 fragments formed detectable levels of protofibrils. Our preliminary studies using Aβ12–40 and Aβ12–40E22G show that the loss of the 1–11 N terminus markedly speeds fibrillization in agreement with other reports,[56] but eliminates the ability to produce protofibrils. So, clearly, mutations affecting amino acid residues in A21, E22 and D23, have dramatic effects on a number of characteristics of Aβ. The Dutch and Iowa variants have been reported to show accelerated kinetics, both for fibrils[17,18,49] and protofibrils,[30] while the Flemish[16] and Italian[17] variants exhibit significantly reduced rates of fibril formation.

The issue of cellular toxicity of Aβ and a number of variants has been addressed. All of the clinically relevant Aβ peptide variants studied in this work have significantly reduced fibril forming rates and been shown to be β-sheet-forming,[18,19] and that β-sheet containing peptide assemblies are able to induce cellular toxicity,[18,49,56–58] with the possible exception of the Italian variant.[17] In transfected cell lines, only the Flemish mutation enhances amyloidogenic processing of βAPP,[18,21] while the Aβ1–42/Aβ1–40 ratio is affected negatively when measured in conditioned media from cells transiently transfected with cDNA coding for mutations generating Aβ1–40E22G, Aβ1–40E22Q or Aβ1–40E22K.[5] The generation of the AβD23N peptide is no different from that of native controls in cell transfection experiments.[18]

The present studies show that: (i) chromatographic studies of Aβ peptides require linear, and not globular, molecular mass standards and high concentrations of salt in the elution buffer are required to overcome deviating behavior in SEC; (ii) the hydrophobicity of the position 22 substituent is a critical determinant of chromatographic behavior but more importantly of nucleation/lag phase length, rate of protofibril and β-sheet formation; (iii) Aβ1–40E22G protofibrillar formation is paralleled by a secondary structural change to β-sheet, thought to be a prerequisite for cellular toxicity.[58] From the parallel SEC and CD studies, we conclude that even smaller oligomeric forms than protofibrils contain β-sheet structure and could therefore be neuotoxic; (iv) the relative thermodynamic stability of the Aβ1–40E22G protofibrils, coupled to their rapid formation, would be an argument for a neutralizing affect on Aβ deposition in brain and would emphasize that potentially more toxic forms of Aβ than fibrils and plaques could build up to destructive levels in the brains of these patients. High concentrations of NaCl, as found in the extracellular space, could promote such a scenario. If diffusion of protofibrils and oligomers in the extracellular space of the brain is significant, damage could be brought upon areas where Aβ production and aggregation is less extensive. Also, with dilution as a consequence of diffusion, the formation of fibrils and plaques would likely be delayed, if the oligomers can maintain their stability (e.g. the Aβ1–40E22G protofibrils or if ADDLs are formed). The issue has been raised of whether the size of the protofibrils is an obstacle for extracellular diffusion to occur in the brain.[59] However, recent findings, using integrative optimal imaging and a cortical slice preparation, show that a large linear polymer of 1057 kDa may move in the extracellular space with the same rate as a small molecule such as tetraethyl ammonium.[60] This means that the mobility of large Aβ intermediates may be much greater in the extracellular space of the brain than previously fathomed. These observations are particularly intriguing in relation to the novel finding of oligomeric Aβ in brains of AD patients.[61,62]

Materials and Methods

Chemicals

Aβ1–40, Aβ1–40E22G, Aβ1–40E22Q, Aβ1–40E22K, Aβ1–40A21G, Aβ1–40E22A, and Aβ1–40E22V were all purchased from Biosource International, Camarillo, CA, USA, while the Aβ12–28 fragments were purchased from Neosystem Laboratories, Strasbourg, France. Molecular mass markers were from Bio-Rad (Bio-Rad Laboratories, USA), aprotinin and bovine serum albumin were from Sigma-Aldrich Chemical Co. (St Louis, USA) and dextran molecular mass standards were from Pharmacosmos (Lyngby, Denmark). All other chemicals were of the highest purity available.

We, and others, have noted that freeze-thawing of

Aβ1–40 peptides can influence their kinetics, most likely due to formation of nuclei. To avoid this, vials were thawed and opened only once, and all peptide used immediately. In this way, the kinetics were kept consistent from one experiment to the other.

Size-exclusion chromatography (SEC)

A Merck Hitachi D-7000 HPLC LaChrom system having a diode array detector (DAD) model L-7455 and a model L-7100 pump was used for the chromatographic analysis. A Superdex 75 PC3.2/30 column (Amersham Biosciences, Uppsala, Sweden) was used for the SEC peptide separation and analysis, unless stated otherwise (see below). The column was eluted with 50 mM phosphate buffer (pH 7.4) with 0.15 M NaCl (PBS) at a flow rate of 0.08 ml/minute (the pressure was 5–6 bar: 1 bar = 10^5 Pa) at ambient temperature (22 °C). All injected samples were subjected to wavelength scan between 200 and 400 nm. Data were extracted from measurements at 214 nm and 280 nm. Peak areas were integrated using Merck Hitachi model D-7000 Chromatography Data Station software. The correlation of the integrated monomeric peak area and peptide concentration was linear ($R^2 = 0.999$) within the peptide concentration range 0–6.46 μg, where all our measurements were carried out.

The monomeric peak integrated area for a range of different peptide concentrations was determined at 214 nm. Each sample was subjected to quantitative amino acid analysis in parallel (PAC, Karolinska Institutet, Stockholm, Sweden) and a standard curve generated where peptide concentration was a function of integrated peak area. With this standard curve we could firmly establish initial concentrations of the peptides in the SEC analyses.

Molecular mass determinations

The globular proteins aprotinin (6.5 kDa), myoglobin (17 kDa), ovalbumin (44 kDa), and bovine serum albumin (66 kDa) were used as molecular mass markers and were run on the three different precision columns 3.2/30; Superdex 75, Superdex 200 and Superose 6. Dextran standards with molecular mass of 21,400, 43, 500, 66,700, 123,600, 196,300, 276,500 and 401,300 Da were applied to the Superdex 75/PC and Superdex 200/PC columns and absorbance was recorded at $A_{275\ nm}$. Plots of elution volume (V_e) *versus* log molecular mass were generated using SigmaPlot Regression Wizard from which molecular mass was calculated for Aβ1–40 and Aβ1–40E22G monomers and protofibrils.

Aβ1–40 static incubation assay/kinetic studies

Prior to incubation, the Aβ1–40 peptides were dissolved in double-distilled water at 5 °C and vortex mixed for two minutes followed by the addition of an equal-volume, double-strength PBS (50 mM sodium phosphate (pH7.4), 0.10 M NaCl). The NaCl was omitted (PB) in samples where SEC results were compared directly with CD data. Tubes with 50 μl of peptide solutions were incubated for various times at 30 °C, protein gene. Incubations were terminated by centrifugation in a fixed-angle rotor using an Eppendorf 5417R centrifuge at 17,900*g* for five minutes (16 °C), where large peptide aggregates were pelleted and separated from soluble peptide remaining in the supernatant. Samples (10 μl) of the supernatant were immediately loaded onto the SEC column.

Experiments using the Aβ12–28 fragments were done in a similar manner but the peptides were studied at a concentration of 100–400 μM and 200 μM was used for the experiments presented in Figure 2 and Table 3. Mass spectrometry confirmed peptide fragment identity and intactness of all fragments even after several months' storage at −20 °C.

Circular dichroism (CD) spectroscopy

Two different spectropolarimeters have been used in the experiments; JASCO-720 with a PTC-343 temperature controller (cells with optical paths of 0.05–0.2 mm), and an AVIV model 62DS spectropolarimeter (Jacksonville, NJ, USA; cell optical path = 0.1 mm). Data points were collected from 250 to 190 nm in 0.5 nm intervals at a rate of 100 nm/minute with one second response time and 20 nm/minute with two seconds response time, respectively. The spectral contribution from the background was subtracted and the results were expressed as mean residual molar ellipticity.

All samples were dissolved at 5 °C in double distilled water, vortex mixed for two minutes, after which one volume of 100 mM phosphate buffer (PB: chloride-free buffer; pH 7.4) was added. Samples were then vortex mixed for another minute but not centrifuged before measurements commenced. CD spectra were recorded at 30 °C with a 0.2 mm optical path length.

Acknowledgements

We thank Dr Magnus Palmblad for his valuable comments on the manuscript, Dr Lars Tjernberg for helping us with mass spectrometry analysis of the Aβ12–28 peptide fragments, and Dr Rudolf Kaiser for valuable technical support on size-exclusion chromatography.

References

1. Hendriks, L., van Duijn, C. M., Cras, P., Cruts, M., Van Hul, W., van Harskamp, F. *et al.* (1992). Presenile dementia and cerebral haemorrhage linked to a mutation at codon 692 of the beta-amyloid precursor protein gene. *Nature Genet.* **1**, 218–221.
2. Levy, E., Carman, M. D., Fernandez-Madrid, I. J., Power, M. D., Lieberburg, I., van Duinen, S. G. *et al.* (1990). Mutation of the Alzheimer's disease amyloid gene in hereditary cerebral hemorrhage, Dutch type. *Science*, **248**, 1124–1126.2.
3. Van Broeckhoven, C., Haan, J., Bakker, E., Hardy, J. A., Van Hul, W., Wehnert, A. *et al.* (1990). Amyloid beta protein precursor gene and hereditary cerebral hemorrhage with amyloidosis (Dutch). *Science*, **248**, 1124–1126.
4. Rossi, G., Macchi, G., Porro, M., Giaccone, G., Bugiani, M., Scarpini, E. *et al.* (1998). Fatal familial insomnia: genetic, neuropathologic, and biochemical study of a patient from a new Italian kindred. *Neurology*, **50**, 688–692.
5. Nilsberth, C., Westlind-Danielsson, A., Eckman, C. B., Condron, M. M., Axelman, K., Forsell, C. *et al.* (2001).

The Arctic APP mutation (E693G) causes Alzheimer's disease by enhanced Aβ protofibril formation. *Nature Neurosci.* **4**, 887–893.
6. Grabowski, T. J., Cho, H. S., Vonsattel, J. P., Rebeck, G. W. & Greenberg, S. M. (2001). Novel amyloid precursor protein mutation in an Iowa family with dementia and severe cerebral amyloid angiopathy. *Ann. Neurol.* **49**, 697–705.
7. Natte, R., Maat-Schieman, M. L., Haan, J., Bornebroek, M., Roos, R. A. & van Duinen, S. G. (2001). Dementia in hereditary cerebral hemorrhage with amyloidosis—Dutch type is associated with cerebral amyloid angiopathy but is independent of plaques and neurofibrillary tangles. *Ann. Neurol.* **50**, 765–772.
8. Kumar-Singh, S., Cras, P., Wang, R., Kros, J. M., van Swieten, J., Lubke, U. *et al.* (2002). Dense-core senile plaques in the Flemish variant of Alzheimer's disease are vasocentric. *Am. J. Pathol.* **161**, 507–520.
9. Shin, Y., Cho, H. S., Fukumoto, H., Shimizu, T., Shirasawa, T., Greenberg, S. M. & Rebeck, G. W. (2003). Abeta species, including IsoAsp23 Abeta, in Iowa-type familial cerebral amyloid angiopathy. *Acta Neuropathol. (Berl)*, **105**, 252–258.
10. Castano, E. M., Prelli, F., Soto, C., Beavis, R., Matsubara, E., Shoji, M. & Frangione, B. (1996). The length of amyloid-beta in hereditary cerebral hemorrhage with amyloidosis, Dutch type. Implications for the role of amyloid-beta 1–42 in Alzheimer's disease. *J. Biol. Chem.* **271**, 32185–32191.
11. Ozawa, K., Tomiyama, T., Maat-Schieman, M. L., Roos, R. A. & Mori, H. (2002). Enhanced Abeta40 deposition was associated with increased Abeta42–43 in cerebral vasculature with Dutch-type hereditary cerebral hemorrhage with amyloidosis (HCHWA-D). *Ann. NY Acad. Sci.* **977**, 149–154.
12. Maat-Schieman, M. L., van Duinen, S. G., Bornebroek, M., Haan, J. & Roos, R. A. (1996). Hereditary cerebral hemorrhage with amyloidosis-Dutch type (HCHWA-D). II. A review of histopathological aspects. *Brain Pathol.* **6**, 115–120.
13. Maat-Schieman, M. L., Radder, C. M., van Duinen, S. G., Haan, J. & Roos, R. A. (1994). Hereditary cerebral hemorrhage with amyloidosis (Dutch): a model for congophilic plaque formation without neurofibrillary pathology. *Acta Neuropathol. (Berl)*, **88**, 371–378.
14. Wisniewski, T., Ghiso, J. & Frangione, B. (1991). Peptides homologous to the amyloid protein of Alzheimer's disease containing a glutamine for glutamic acid substitution have accelerated amyloid fibril formation. *Biochem. Biophys. Res. Commun.* **179**, 1247–1254.
15. Fraser, P. E., Nguyen, J. T., Inouye, H., Surewicz, W. K., Selkoe, D. J., Podlisny, M. B. & Kirschner, D. A. (1992). Fibril formation by primate, rodent, and Dutch-hemorrhagic analogues of Alzheimer amyloid beta-protein. *Biochemistry*, **31**, 10716–10723.
16. Walsh, D. M., Hartley, D. M., Condron, M. M., Selkoe, D. J. & Teplow, D. B. (2001). *In vitro* studies of amyloid beta-protein fibril assembly and toxicity provide clues to the aetiology of Flemish variant (Ala692 → Gly) Alzheimer's disease. *Biochem. J.* **355**, 869–877.
17. Miravalle, L., Tokuda, T., Chiarle, R., Giaccone, G., Bugiani, O., Tagliavini, F. *et al.* (2000). Substitutions at codon 22 of Alzheimer's abeta peptide induce diverse conformational changes and apoptotic effects in human cerebral endothelial cells. *J. Biol. Chem.* **275**, 27110–27116.
18. Van Nostrand, W. E., Melchor, J. P., Cho, H. S., Greenberg, S. M. & Rebeck, G. W. (2001). Pathogenic effects of D23N Iowa mutant amyloid beta-protein. *J. Biol. Chem.* **276**, 32860–32866.
19. Kirkitadze, M. D., Condron, M. M. & Teplow, D. B. (2001). Identification and characterization of key kinetic intermediates in amyloid beta-protein fibrillogenesis. *J. Mol. Biol.* **312**, 1103–1119.
20. Haass, C., Hung, A. Y., Selkoe, D. J. & Teplow, D. B. (1994). Mutations associated with a locus for familial Alzheimer's disease result in alternative processing of amyloid beta-protein precursor. *J. Biol. Chem.* **269**, 17741–17748.
21. Stenh, C., Nilsberth, C., Hammarback, J., Engvall, B., Naslund, J. & Lannfelt, L. (2002). The Arctic mutation interferes with processing of the amyloid precursor protein. *Neuroreport*, **13**, 1857–1860.
22. Tsubuki, S., Takaki, Y. & Saido, T. C. (2003). Dutch, Flemish, Italian, and Arctic mutations of APP and resistance of Abeta to physiologically relevant proteolytic degradation. *Lancet*, **361**, 1957–1958.
23. Monro, O. R., Mackic, J. B., Yamada, S., Segal, M. B., Ghiso, J., Maurer, C. *et al.* (2002). Substitution at codon 22 reduces clearance of Alzheimer's amyloid-beta peptide from the cerebrospinal fluid and prevents its transport from the central nervous system into blood. *Neurobiol. Aging*, **23**, 405–412.
24. Wang, Z., Natte, R., Berliner, J. A., van Duinen, S. G. & Vinters, H. V. (2000). Toxicity of Dutch (E22Q) and Flemish (A21G) mutant amyloid beta proteins to human cerebral microvessel and aortic smooth muscle cells. *Stroke*, **31**, 534–538.
25. Davis, J. & Van Nostrand, W. E. (1996). Enhanced pathologic properties of Dutch-type mutant amyloid beta-protein. *Proc. Natl Acad. Sci. USA*, **93**, 2996–3000.
26. Melchor, J. P., McVoy, L. & Van Nostrand, W. E. (2000). Charge alterations of E22 enhance the pathogenic properties of the amyloid beta-protein. *J. Neurochem.* **74**, 2209–2212.
27. Verbeek, M. M., de Waal, R. M., Schipper, J. J. & Van Nostrand, W. E. (1997). Rapid degeneration of cultured human brain pericytes by amyloid beta protein. *J. Neurochem.* **68**, 1135–1141.
28. Nunan, J. & Small, D. H. (2002). Proteolytic processing of the amyloid-beta protein precursor of Alzheimer's disease. *Essays Biochem.* **38**, 37–49.
29. Jarrett, J. T. & Lansbury, P. T., Jr (1993). Seeding one-dimensional crystallization of amyloid: a pathogenic mechanism in Alzheimer's disease and scrapie? *Cell*, **73**, 1055–1058.
30. Walsh, D. M., Lomakin, A., Benedek, G. B., Condron, M. M. & Teplow, D. B. (1997). Amyloid beta-protein fibrillogenesis. Detection of a protofibrillar intermediate. *J. Biol. Chem.* **272**, 22364–22372.
31. Harper, J. D., Wong, S. S., Lieber, C. M. & Lansbury, P. T. (1997). Observation of metastable Abeta amyloid protofibrils by atomic force microscopy. *Chem. Biol.* **4**, 119–125.
32. Lambert, M. P., Barlow, A. K., Chromy, B. A., Edwards, C., Freed, R., Liosatos, M. *et al.* (1998). Diffusible nonfibrillar ligands derived from Abeta1–42 are potent central nervous system neurotoxins. *Proc. Natl Acad. Sci. USA*, **95**, 6448–6453.
33. Stine, W. B., Dahlgren, K. N., Jr, Grant, A., Krafft, G. A. & Mary Jo LaDu, M. J. (2003). *In vitro* characterization of conditions for amyloid-peptide oligomerization and fibrillogenesis. *J. Biol. Chem.* **278**, 11612–11622.

34. Walsh, D. M., Hartley, D. M., Kusumoto, Y., Fezoui, Y., Condron, M. M., Lomakin, A. *et al.* (1999). Amyloid beta-protein fibrillogenesis. Structure and biological activity of protofibrillar intermediates. *J. Biol. Chem.* **274**, 25945–25952.
35. Harper, J. D., Lieber, C. M. & Lansbury, P. T., Jr (1997). Observation of metastable Abeta amyloid protofibrils by atomic force microscopy. *Chem. Biol.* **4**, 951–959.
36. Hartley, D. M., Walsh, D. M., Ye, C. P., Diehl, T., Vasquez, S., Vassilev, P. M. *et al.* (1999). Protofibrillar intermediates of amyloid beta-protein induce acute electrophysiological changes and progressive neurotoxicity in cortical neurons. *J. Neurosci.* **19**, 8876–8884.
37. Ye, C. P., Selkoe, D. J. & Hartley, D. M. (2003). Protofibrils of amyloid beta-protein inhibit specific K^+ currents in neocortical cultures. *Neurobiol. Dis.* **13**, 177–190.
38. Black, S. D. & Mould, D. R. (1991). Development of hydrophobicity parameters to analyze proteins which bear post- or co-translational modifications. *Anal. Biochem.* **193**, 72–82.
39. Hilbich, C., Kisters-Woike, B., Reed, J., Masters, C. L. & Beyreuther, K. (1991). Aggregation and secondary structure of synthetic amyloid beta A4 peptides of Alzheimer's disease. *J. Mol. Biol.* **218**, 149–163.
40. Huang, T. H., Fraser, P. E. & Chakrabartty, A. (1997). Fibrillogenesis of Alzheimer Abeta peptides studied by fluorescence energy transfer. *J. Mol. Biol.* **269**, 214–224.
41. Garzon-Rodriguez, W., Sepulveda-Becerra, M., Milton, S. & Glabe, C. G. (1997). Soluble amyloid Abeta-(1–40) exists as a stable dimer at low concentrations. *J. Biol. Chem.* **272**, 21037–210344.
42. Garzon-Rodriguez, W., Vega, A., Sepulveda-Becerra, M., Milton, S., Johnson, D. A., Yatsimirsky, A. K. & Glabe, C. G. (2000). A conformation change in the carboxyl terminus of Alzheimer's Abeta (1–40) accompanies the transition from dimer to fibril as revealed by fluorescence quenching analysis. *J. Biol. Chem.* **275**, 22645–22649.
43. Palmblad, M., Westlind-Danielsson, A. & Bergquist, J. (2002). Oxidation of methionine 35 attenuates formation of amyloid beta-peptide 1–40 oligomers. *J. Biol. Chem.* **277**, 19506–19510.
44. Dobeli, H., Draeger, N., Huber, G., Jakob, P., Schmidt, D., Seilheimer, B. *et al.* (1995). A biotechnological method provides access to aggregation competent monomeric Alzheimer's 1–42 residue amyloid peptide. *Biotechnol. (NY)*, **13**, 988–993.
45. Tseng, B. P., Esler, W. P., Clish, C. B., Stimson, E. R., Ghilardi, J. R., Vinters, H. V. *et al.* (1999). Deposition of monomeric, not oligomeric, Abeta mediates growth of Alzheimer's disease amyloid plaques in human brain preparations. *Biochemistry*, **38**, 10424–10431.
46. Lee, S., Suh, Y. H., Kim, S. & Kim, Y. (1999). Comparison of the structures of beta amyloid peptide (25–35) and substance P in trifluoroethanol/water solution. *J. Biomol. Struct. Dynam.* **17**, 381–391.
47. Danielsson, J., Jarvet, J., Damberg, P. & Gräslund, A. (2002). Translational diffusion measured by PFG-NMR on full length and fragments of the Alzheimer Aβ(1–40) peptide. Determination of hydrodynamic radii of random coil peptides of varying length. *Magn. Reson. Chem.* **40**, 589–597.
48. Curtain, C. C., Ali, F., Volitakis, I., Cherny, R. A., Norton, R. S., Beyreuther, K. *et al.* (2001). Alzheimer's disease amyloid-beta binds copper and zinc to generate an allosterically ordered membrane-penetrating structure containing superoxide dismutase-like subunits. *J. Biol. Chem.* **8**, 20466–22047.
49. Sian, A. K., Frears, E. R., El-Agnaf, O. M., Patel, B. P., Manca, M. F., Siligardi, G. *et al.* (2000). Oligomerization of beta-amyloid of the Alzheimer's and the Dutch-cerebral-haemorrhage types. *Biochem. J.* **349**, 299–308.
50. Jarvet, J., Damberg, P., Danielsson, J., Johansson, I., Eriksson, L. E. G. & Gräslund, A. (2003). A left-handed 3_1 helical conformation in the Alzheimer Aβ(12–28) peptide. *FEBS Letters*, **555**, 371–374.
51. Fraser, P. E., Nguyen, J. T., Surewicz, W. K. & Kirschner, D. A. (1991). pH-dependent structural transitions of Alzheimer amyloid peptides. *Biophys. J.* **60**, 1190–1201.
52. Fraser, P. E., McLachlan, D. R., Surewicz, W. K., Mizzen, C. A., Snow, A. D., Nguyen, J. T. & Kirschner, D. A. (1994). Conformation and fibrillogenesis of Alzheimer A beta peptides with selected substitution of charged residues. *J. Mol. Biol.* **244**, 64–73.
53. Gorevic, P. D., Castano, E. M., Sarma, R. & Frangione, B. (1987). Ten to fourteen residue peptides of Alzheimer's disease protein are sufficient for amyloid fibril formation and its characteristic Xray diffraction pattern. *Biochem. Biophys. Res. Commun.* **147**, 854–862.
54. Kirschner, D. A., Inouye, H., Duffy, L. K., Sinclair, A., Lind, M. & Selkoe, D. J. (1987). Synthetic peptide homologous to beta protein from Alzheimer disease forms amyloid-like fibrils *in vitro*. *Proc. Natl Acad. Sci. USA*, **84**, 6953–6957.
55. Jarvet, J., Damberg, P., Bodell, K., Eriksson, L. E. G. & Graslund, A. (2000). Reversible random coil to β-sheet transition and the early stage of aggregation of the Aβ(12–28) fragment from the Alzheimer peptide. *J. Am. Chem. Soc.* **122**, 4261–4268.
56. Jarrett, J. T., Berger, E. P. & Lansbury, P. T., Jr (1993). The carboxy terminus of the beta amyloid protein is critical for the seeding of amyloid formation: implications for the pathogenesis of Alzheimer's disease. *Biochemistry*, **32**, 4693–4697.
57. Walsh, D. M., Hartley, D. M., Condron, M. M., Selkoe, D. J. & Teplow, D. B. (2001). *In vitro* studies of amyloid beta-protein fibril assembly and toxicity provide clues to the aetiology of Flemish variant (Ala692– > Gly) Alzheimer's disease. *Biochem. J.* **355**, 869–877.
58. Harkany, T., Abraham, I., Konya, C., Nyakas, C., Zarandi, M., Penke, B. & Luiten, P. G. (2000). Mechanisms of beta-amyloid neurotoxicity: perspectives of pharmacotherapy. *Rev. Neurosci.* **11**, 329–382.
59. Roher, A. E., Baudry, J., Chaney, M. O., Kuo, Y. M., Stine, W. B. & Emmerling, M. R. (2000). Oligomerizaiton and fibril asssembly of the amyloid-beta protein. *Biochim. Biophys. Acta*, **1502**, 31–43.
60. Prokopova-Kubinova, S., Vargova, L., Tao, L., Ulbrich, K., Subr, V., Sykova, E. & Nicholson, C. (2001). Poly[*N*-(2-hydroxypropyl)methacrylamide] polymers diffuse in brain extracellular space with same tortuosity as small molecules. *Biophys. J.* **80**, 542–548.
61. Gong, Y., Chang, L., Viola, K. L., Lacor, P. N., Lambert, M. P., Finch, C. E. *et al.* (2003). Alzheimer's disease-affected brain: presence of oligomeric A beta ligands (ADDLs) suggests a molecular basis for

reversible memory loss. *Proc. Natl Acad. Sci. USA*, **100**, 10417–10422.
62. Kayed, R., Head, E., Thompson, J. L., McIntire, T. M., Milton, S. C., Cotman, C. W. & Glabe, C. G. (2003). Common structure of soluble amyloid oligomers implies common mechanism of pathogenesis. *Science*, **300**, 486–489.

Edited by A. Klug

(Received 24 October 2003; received in revised form 11 February 2004; accepted 12 March 2004)